Systematic measurement of the relative electron-impact excitation cross section of the $3d \rightarrow 2p\ ^1P_1$ resonance and $^3D_1$ intercombination lines in mid-Z neonlike ions

G. V. Brown, P. Beiersdorfer, and K. Widmann
Department of Physics, Lawrence Livermore National Laboratory, Livermore, California 94551
(Received 18 September 2000; published 15 February 2001)

The relative electron-impact cross sections for exciting the $3d \rightarrow 2p\ ^1P_1$ resonance and $^3D_1$ intercombination lines have been measured in nine neonlike ions between Cr^{14+} and Kr^{26+}. The ratio drops from about 4.4 for Cr^{14+} to less than unity for Kr^{26+} in response to an increase in relativistic effects. A measurement of the dependence of this ratio on electron energy is presented for Fe^{16+}. No dependence on electron energy is found. The measured ratios are generally lower than theory, showing that the relative intensity of the intercombination line is larger than predicted and illustrating the difficulty to predict electron-impact excitation cross sections in the intermediate coupling regime at the level needed for spectral diagnostics.

DOI: 10.1103/PhysRevA.63.032719 PACS number(s): 34.50.Gb, 32.30.Rj, 32.30.−r, 32.70.Fw

I. INTRODUCTION

The calculation of electron-impact excitation cross sections of highly charged ions at the level of accuracy needed for reliable plasma diagnostics remains a challenge for multielectron ions. Even for relatively simple ions, such as ten-electron neonlike ions where the $1s^2 2s^2 2p^6$ ground configuration consists of completely filled shells, predictions utilizing different theoretical approaches can easily differ by factors of 2. By contrast, experiments, especially those involving observations of extraterrestrial sources, x-ray lasers, and inertial confinement research, demand accuracies better than 10%.

The need for accurate calculations was recently stressed in the case of the $2p^5 3d_{3/2}\ ^1P_1 \rightarrow 2p^6\ ^1S_0$ and $2p^5 3d_{5/2}\ ^3D_1 \rightarrow 2p^6\ ^1S_0$ resonance and intercombination lines in neonlike ions, known as $3C$ and $3D$, respectively [1,2]. The two lines are among the strongest, most distinct $n=3 \rightarrow n=2$ L-shell spectral features in mid-Z neonlike ions. In addition to their strong brightness, they have several properties that make them attractive diagnostic candidates. In the coronal limit, the dominant excitation process for each line is by far collisional excitation from the ground state, and there are no competing radiative or autoionizing decay channels. This means that excitation models need only concentrate on accurate predictions of the electron-impact excitation cross sections. Accurate measurement of their relative intensities is helped by the fact that the lines are close to one another in wavelength, making it easy to measure both lines simultaneously and to accurately account for response effects of the measuring instrument.

The spectral features produced by neonlike transitions have been investigated for diagnosing extraterrestrial sources such as the Sun [1–5], stellar coronae [6,7], and x-ray binaries [8], as well as terrestrial sources including tokamaks [9–11] and laser-produced plasmas [12,13]. One specific diagnostic that has been pursued is a density diagnostic based on resonant fluorescence, commonly referred to as resonant scattering, of the $3C$ resonance line relative to the $3D$ intercombination line. In the case of Fe^{16+}, resonant scattering has been used to infer density, column density, and path length of active regions in the Sun using a method described by several authors [14–17]. This method relies explicitly on the optically thin intensity ratio, where neither line is resonantly scattered, to infer an optical depth of the $3C$ line [18]. Calculations of the optically thin value have been produced by several authors [19–27]. A closer look at the results from these calculations, however, shows that there is scatter by about a factor of 2 among the relative excitation cross sections of the intercombination and resonance line, which effectively eliminates the utility of the line pair as a plasma diagnostic. The difficulty in calculating the intensity ratios of the two neonlike lines is caused in part by the fact that relativity plays a strong role in the description of these mid-Z ions. As Z increases, LS-coupling gives way to jj-coupling, and the intercombination line increases in intensity at the expense of the resonance line. In fact, near $Z=38$ the two lines are predicted to have equal collision strengths [28] and thus equal intensities. The Fe^{16+} ion is located in the middle of this changeover, and intermediate coupling is paramount for an accurate description of this ion.

The difficulty in properly describing the relative cross sections of lines $3C$ and $3D$ in Fe^{16+} indicates a strong need for definitive experimental data. In the case of Fe^{16+}, we have recently provided such data [29] and shown that the actual ratio is $\approx 25\%$ less than the most recent calculation. In the following, we present a set of measurements that can be used as benchmarks for testing theoretical models of the relative cross section of the two lines as a function of atomic number Z. In the case of Fe^{16+}, we present in addition a measurement of the relative electron-impact excitation cross sections as a function of electron energy. This measurement shows that the ratio is independent of the excitation energy. The $3C$ to $3D$ ratios measured for all nine neonlike ions given here are lower than predicted and match predictions from distorted-wave calculations only if the nuclear charge for each ion in the calculation were reduced by about 2.

II. EXPERIMENTAL ARRANGEMENT

The measurements were conducted using the EBIT-II electron beam ion trap located at the Lawrence Livermore National Laboratory. EBIT-II operates at energies below 24 keV

and has been extensively used for observations in the realm of x-ray, EUV, UV, and optical spectroscopy. Overviews of spectroscopic efforts conducted on EBIT-II are provided by Beiersdorfer *et al.* [30,31], and a review of the Livermore electron beam ion traps is given by Marrs [32]. In brief, the target material under investigation was injected into the trap region, where it was trapped electrostatically by applied voltages in the axial direction and by the charge of the electron beam in the radial direction. Once trapped, the target material was then collisionally ionized to the desired charge state by the monoenergetic electron beam and its emission was studied using a spectrometer arrangement appropriate to the photon energy and desired resolution. There were two devices used to inject the target material into the trap region: the metal vapor vacuum arc (MeVVA) and the gas injector. The MeVVA injected singly or doubly ionized ions into the trap electrostatically, while the gas injector, using differential pumping, sends a constant stream of neutrals directly into the trap. The method of injection depends on the natural state of the element being studied.

Line emission presented here was measured using one of two flat crystal spectrometers, referred to as the BRAD-I and the BRAD-II [33,34], which look directly into the trap region perpendicular to the electron beam. These spectrometers used flat crystals to disperse x rays according to Bragg's Law [35]. For the present measurements, either a thallium acid phthalate (TlAP; $2d=25.757$ Å [36]) or a rubidium acid phthalate (RAP; $2d=26.121$ Å [36]) crystal was employed. Once dispersed, the x rays were detected by a position-sensitive proportional counter [37]. The resolving power of the spectrometers was limited by the crystals and was $\lambda/\Delta\lambda \cong 300-1000$.

In order to effectively eliminate the absorption of x rays, the spectrometers operated at a pressure of $\sim 10^{-5}$ torr. The vacuum of EBIT-II was on the order of 10^{-10} torr, consequently it was necessary to provide a barrier between the spectrometer and EBIT-II in order to preserve the integrity of EBIT-II's vacuum. This barrier was provided by a 25-mm-diam$\times$1.0-μm thick polyimide window for BRAD-I, and a 25-mm-diam$\times$0.5-μm-thick mylar window for BRAD-II. In addition to these windows, the proportional counters each utilized a 4-μm-thick polypropylene window coated with 200–400 Å of aluminum to isolate their detection chamber ($P=760$ torr of $P-10$) from the chamber of the spectrometer.

III. MEASUREMENT

The measured spectra of the $3C$ resonance to $3D$ intercombination lines along the neonlike isoelectronic sequence between Cr^{14+} and Kr^{26+} are shown in Figs. 1–3. The electron beam energy at which each spectrum was taken was chosen such that it was well above the ionization energy to create the neonlike ion and just slightly below the energy to create the fluorinelike ion (cf. Table I). This not only insured a nearly pure neonlike charge state, but also limited the line population processes to direct impact excitation from the ground state and radiative cascades from levels of higher principal quantum number, n. In the case of Fe^{16+}, we also

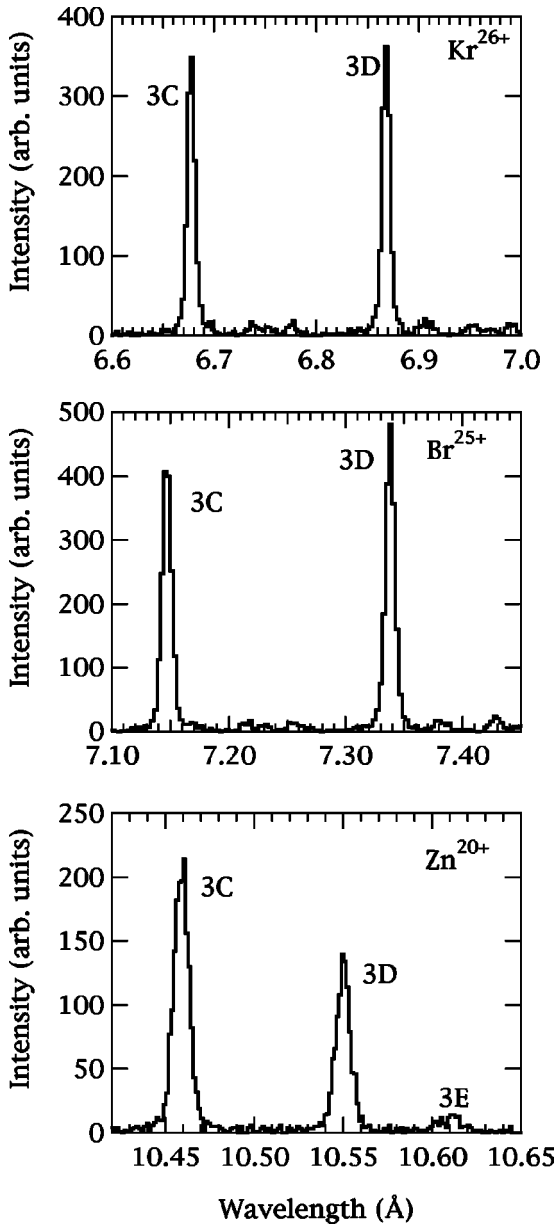

FIG. 1. Measured neonlike spectra of Kr^{26+}, Br^{25+}, and Zn^{20+}. $3E$ denotes the transition $2p^5 3d_{3/2}\,{}^3P_1 \rightarrow 2p^6\,{}^1S_0$.

measured this ratio as a function of energy from slightly above threshold to 4 keV. These results are shown in Fig. 4.

Because EBIT-II employs a unidirectional electron beam, it creates line emission that is linearly polarized [38]. Also, the crystals used in this experiment act as polarimeters, and therefore reflect the parallel and perpendicular electron field component differently [36,38]. The relative polarization of the resonance line and the intercombination line is calculated to differ by less than 0.3% at energies between threshold and 4 keV [39]; hence, the effect of the directionality of the beam is the same for both lines. By taking the ratio of the lines, the polarization effects cancel making it unnecessary to account for polarization in our analysis in any other way.

As is seen in Table I, different crystals were used for different neonlike ions. This was done in order to avoid the absorption edges of the crystals. For example, thallium has

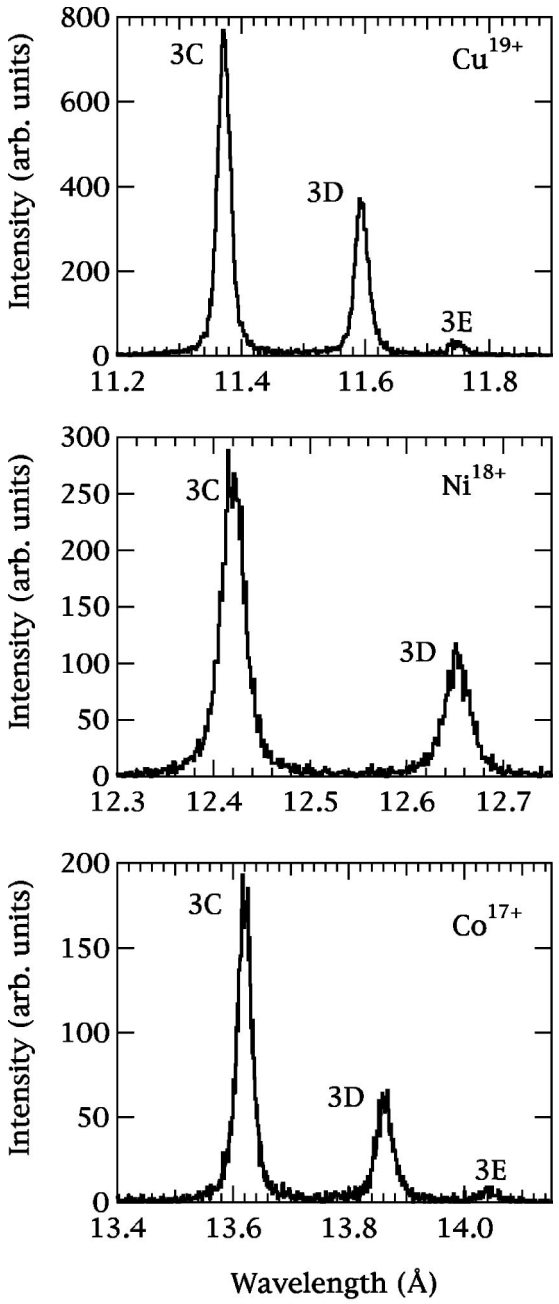

FIG. 2. Measured neonlike spectra of Cu^{19+}, Ni^{18+}, and Co^{17+}.

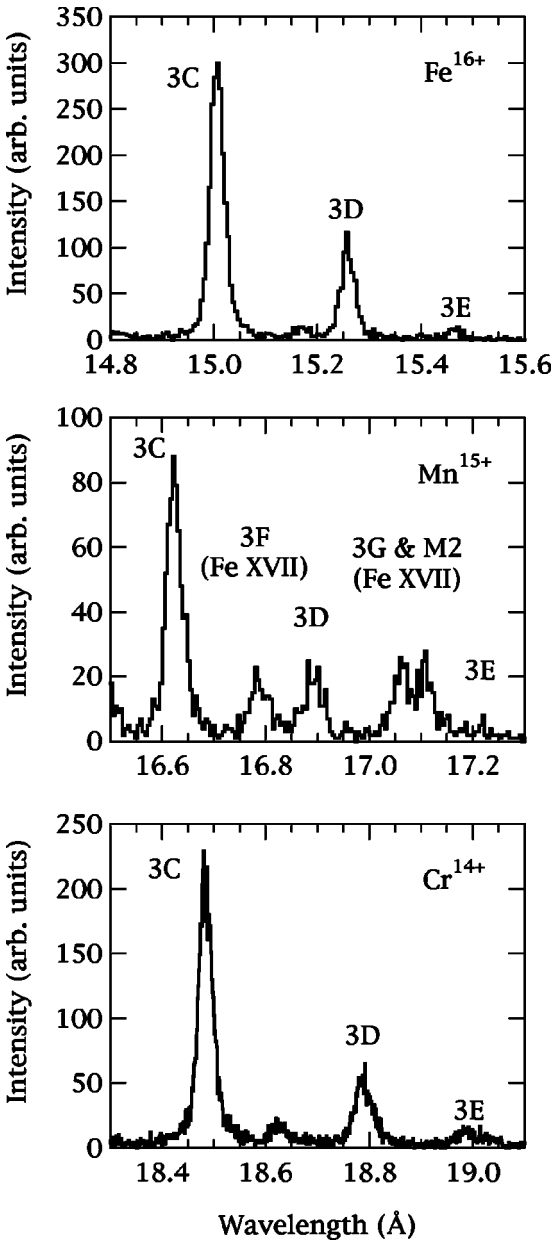

FIG. 3. Measured neonlike spectra of Fe^{16+}, Mn^{15+}, and Cr^{14+}. $3F$, $3G$, and $M2$ denote the transitions $2p^5 3s\ ^3P_1$, $^3P_1$, and $^3P_2 \rightarrow 2p^6\ ^1S_0$, respectively.

N-shell absorption edges in this energy band at 846 eV (14.7 Å) and 720 eV (17.2 Å), and rubidium has *L*-shell absorption edges in this energy band at 1864 eV (6.6 Å) [40]. It is our experience that the reflectivity of the TlAP is higher than RAP, hence, in the regions where neither crystal has an absorption edge, TlAP was used.

IV. RESULTS AND DISCUSSION

The results of the measurements of the relative collision strengths of $3C$ and $3D$ versus Z are shown in Fig. 5 and tabulated in Table II. The measured ratios have been corrected for instrumental response, which includes the effects of all polymer windows on both the spectrometer and on the detector, as well as the reflection properties of the crystals [40]. The error bars include the statistical uncertainty from each line and the estimated uncertainty in the instrumental response. It is noted that although some spectra do exhibit emission from ions other than the target ion, this emission is resolved from the lines of interest and, therefore, has no effect on the ratios presented here. For example, the Mn^{15+} spectrum (see Fig. 3) contains a significant amount of Fe^{16+} emission because the MeVVA employed to inject manganese utilized an iron trigger wire. The Fe^{16+} emission is well resolved and has no effect on the Mn^{15+} $3C$ to $3D$ ratio.

We compare our measurements of this ratio versus Z with the relative collision strengths of the fully relativistic

TABLE I. Parameters of measurements and properties of the $2p^5 3d_{3/2}\,{}^1P_1 \rightarrow 2p^6\,{}^1S_0$ resonance and $2p^5 3d_{5/2}\,{}^3D_1 \rightarrow 2p^6\,{}^1S_0$ intercombination line. E^{Ne} and E^{F} are the electron-impact energies necessary to make the neonlike and fluorinelike ions, respectively.

Ion	$\lambda_{^1P_1}$ (Å) [a]	$\lambda_{^3D_1}$ (Å) [a]	Crystal	Foils [b]	E^{Ne}	E^{F}	E (eV) [c]
Cr^{14+}	18.5019	18.7971	RAP	*A*	384 eV	1010 eV	960 eV
Mn^{15+}	16.6236	16.8956	RAP	*A*	436 eV	1133 eV	1030 eV
Fe^{16+}	15.014(1)	15.261(2)	RAP	*A*	489 eV	1265 eV	1150 eV
Co^{17+}	13.6350	13.8725	TlAP	*A*	547 eV	1397 eV	1320 eV
Ni^{18+}	12.4340	12.6589	TlAP	*A*	607 eV	1540 eV	1470 eV
Cu^{19+}	11.3843	11.5990	TlAP	*A*	671 eV	1690 eV	1600 eV
Zn^{21+}	10.4613	10.6678	RAP	*A*	737 eV	1846 eV	1700 eV
Br^{35+}	7.17002	7.35375	TlAP [d]	*B*	1119 eV	2730 eV	2625 eV
Kr^{36+}	6.69816	6.87954	TlAP [d]	*B*	1205 eV	2927 eV	2827 eV

[a]All wavelengths are those of [45] except Fe^{16+}, which was measured by Brown *et al.* 1998 [29].
[b]$A = 4\,\mu$m polypropylene plus 0.5 μm mylar; $B = 4\,\mu$m polypropylene plus 1 μm polyimide.
[c]Electron energy at which ratio was measured.
[d]Second-order measurement.

distorted-wave model of Zhang and Sampson [28] and with a calculation by Hibbert *et al.* [41], who use the configuration-interaction method (see Fig. 5). Because Hibbert calculates weighted oscillator strengths, it is necessary to divide his calclulation by the transition energy before comparing with our measurements. The correction to the ratio is only 2–3 % because the energy separation of the $3C$ and $3D$ lines is minimal. With the exception of Cr^{14+} and Mn^{15+}, both theories agree with one another and also both the theories and the experiment are smoothly decreasing functions of Z.

As mentioned in Sec. I, the decrease in the line intensity ratio is a result of the fact that relativity plays an increasing role, i.e., the dominant interaction energy is changing from the electrostatic interaction to the spin-orbit interaction. Although all three curves have nearly the same Z dependence ($\propto 1/Z^4$), there is a systematic shift between each of the calculations and the experiment of $\sim 30\%$. This difference corresponds to fitting the curve with a shifted $Z_{\mathrm{eff}} = Z - 2$. Even larger differences can be noted with other calculations, e.g., Bhatia *et al.* show a discrepancy of nearly 60% in the case of Fe^{16+} and a factor of 3.6 in the case of Cr^{14+} [21].

We note that the ratio continues to decrease as a function of Z beyond $Z = 36$. This is demonstrated by previous measurements of higher-Z neonlike ions. For example, Beiersdorfer [11] gives a value of 0.63 ± 0.19 for Ag^{37+} and a measurement by Marrs *et al.* of Ba^{46+} gives a value of 0.55 ± 0.11 [42].

The energy dependence of the Fe^{16+} measurement is compared to the *R*-matrix model of Mohan *et al.* [27], the results of Bhatia and Doschek [25] , and the distorted-wave calculations of Zhang and Sampson [28] (see Fig. 4). These

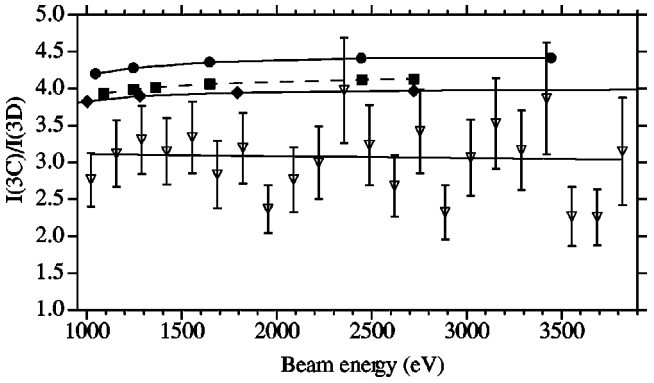

FIG. 4. Ratio R of Fe^{16+} $2p^5 3d_{3/2}\,{}^1P_1 \rightarrow 2p^6\,{}^1S_0$ ($3C$) and $2p^5 3d_{5/2}\,{}^3D_1 \rightarrow 2p^6\,{}^1S_0$ ($3D$) as a function of energy. The measurement is depicted by inverted triangles, filled squares are the *R*-matrix calculation of Mohan *et al.* [27], filled circles depict the calculation of Bhatia and Doschek [25], and the filled diamonds depict the relativistic distorted-wave calculation of Zhang and Sampson [28]. We also show a weighted linear fit to our data. In the region above threshold shown here, the average value for the ratio, R, is 3.04 ± 0.19. This is corrected for instrumental response including foil and crystal transmission and reflectivity.

TABLE II. Measured and calculated relative cross sections of the $^1P_1$ resonance and $^3D_1$ intercombination line for neonlike ions between Cr^{14+} and Kr^{26+}

Z	Measured ratio	Zhang and Sampson[a]	Hibbert *et al.*[b]
24	4.37 ± 0.43	5.54	4.77
25	3.42 ± 0.30	4.62	4.07
26	3.04 ± 0.12	3.90	3.83
27	2.59 ± 0.18	3.31	3.28
28	2.30 ± 0.16	2.86	2.83
29	1.97 ± 0.14	2.44	2.47
30	1.71 ± 0.10	2.15	2.17
31		1.90	1.93
32		1.70	1.74
33		1.53	1.58
34		1.40	1.44
35	0.93 ± 0.07	1.28	1.34
36	0.99 ± 0.07	1.19	1.25

[a]Reference [28].
[b]Reference [41].

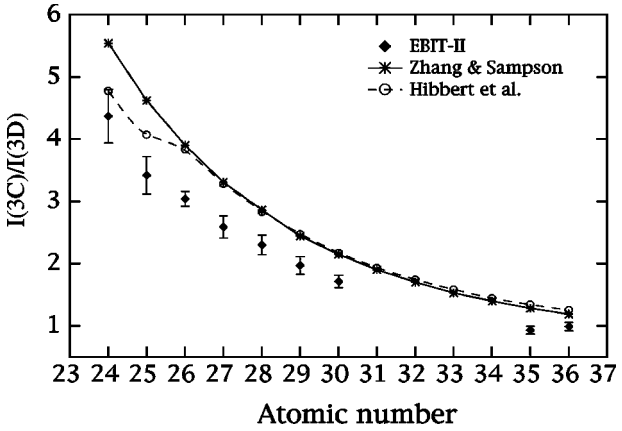

FIG. 5. Results of the present measurement, labeled EBIT-II, compared to calculations of Hibbert *et al.* [42] and Zhang and Sampson. All three curves scale as $1/Z^4$; however, there is a systematic shift of ~30% between both theories and the experimental data.

results, both experimental and theoretical, show that this ratio has no energy dependence. The lack of energy dependence of the ratio has been measured and predicted in other neonlike ions [43,42]. Of course, the predicted value from all these authors is considerably higher than measured.

The fact that the ratio is independent of energy above threshold means that the ratio is unchanged when averaged over any electron energy distribution function. Our measurements, conducted at single electron beam energies, are therefore equivalent to relative electron-impact rate coefficient measurements in a plasma with a Maxwellian or even non-Maxwellian electron temperature. Therefore, our results also present benchmarks for testing calculations of relative rate coefficients used for plasma diagnostics.

In conclusion, we find a systematic difference for the relative excitation cross sections of the neonlike $3d \rightarrow 2p$ resonance and intercombination line over a range of Z where intermediate coupling is required to describe the wave functions. The present results confirm the discrepancy between theory and experiment found earlier for Fe^{16+} [29] and extend it along the isoelectronic sequence. In all cases, the relative strength of the intercombination line is found to be larger than predicted. The present result is thus qualitatively the same as that for the ratio of intercombination to the resonance line in mid-Z heliumlike ions reported recently [44]. Calculations provide good agreement with the measurements only if the effective atomic number is shifted by about two units.

ACKNOWLEDGMENTS

We are happy to acknowledge the dedicated technical support of Dan Nelson, Ken Visbeck, and Phil D'Antonio. The author would also like to thank E. Träbert for his helpful comments on atomic theory and K. Reed for his calculations. This work was performed under the auspices of the U.S. Department of Energy by the University of California Lawrence Livermore National Laboratory under Contract No. W-7405-Eng-48 and was supported by a grant from NASA's Space Astrophysics Research and Analysis Program.

[1] J.H. Parkinson, Astron. Astrophys. **24**, 215 (1973).
[2] M. Loulergue and H. Nussbaumer, Astron. Astrophys. **45**, 125 (1975).
[3] D.L. McKenzie and P.B. Landecker, Astrophys. J. **254**, 309 (1982).
[4] K.J.H. Phillips *et al.*, Astrophys. J. **256**, 774 (1982).
[5] H.R. Rugge and D.L. McKenzie, Astrophys. J. **297**, 338 (1985).
[6] P.W. Vedder and C.R. Canizares, Astrophys. J. **270**, 666 (1983).
[7] A.C. Brinkman *et al.*, Astrophys. J. Lett. **530**, L111 (2000).
[8] S.M. Kahn, F.D. Seward, and T. Chlebowski, Astrophys. J. **283**, 286 (1984).
[9] S. von Goeler *et al.*, *X-ray Spectroscopy on Tokamaks*, in *Diagnostics for Fusion Reactor Conditions*, edited by P. Scott *et al.* (Commission of the European Communities, Belgium, 1982), p. 109.
[10] E. Källne, J. Källne, E. Marmar, and J. Rice, Phys. Scr. **31**, 551 (1985).
[11] P. Beiersdorfer, Ph.D. thesis, Princeton University, 1988.
[12] C.J. Keane *et al.*, Phys. Fluids B **5**, 3328 (1993).
[13] S.Y. Khakhalin *et al.*, Phys. Scr. **50**, 102 (1994).
[14] L.W. Acton, Astrophys. J. **225**, 1069 (1978).
[15] K. Waljeski *et al.*, Astrophys. J. **429**, 909 (1994).
[16] J.T. Schmelz, J.L.R. Saba, J.C. Chauvin, and K.T. Strong, Astrophys. J. **477**, 509 (1997).
[17] J.L.R. Saba, J.T. Schmelz, A.K. Bhatia, and K.T. Strong, Astrophys. J. **510**, 1064 (1999).
[18] S.O. Kastner and R.E. Kastner, J. Quant. Spectrosc. Radiat. Transf. **44**, 275 (1990).
[19] A. Bely and F. Bely, Sol. Phys. **2**, 285 (1967).
[20] J.B. Mann, At. Data Nucl. Data Tables **29**, 307 (1983).
[21] A.K. Bhatia, U. Feldman, and J.F. Seely, At. Data Nucl. Data Tables **32**, 435 (1985).
[22] B.W. Smith, J.C. Raymond, J.B. Mann, and R.D. Cowan, Astrophys. J. **298**, 898 (1985).
[23] P.L. Hagelstein and R.K. Jung, At. Data Nucl. Data Tables **37**, 121 (1987).
[24] H.L. Zhang, D.H. Sampson, R.E.H. Clark, and J.B. Mann, At. Data Nucl. Data Tables **37**, 17 (1987).
[25] A.K. Bhatia and G.A. Doschek, At. Data Nucl. Data Tables **52**, 1 (1992).
[26] M. Cornille, J. Dubau, P. Faucher, F. Bely-Dubau, and C. Blanchard, Astron. Astrophys. **105**, 77 (1994).
[27] M. Mohan, R. Sharma, and W. Eissner, Astrophys. J. **108**, 389 (1997).
[28] H.L. Zhang, D. Sampson, and A.K. Mohanty, Phys. Rev. A **40**, 616 (1989).
[29] G.V. Brown *et al.*, Astrophys. J. **502**, 1015 (1998).
[30] P. Beiersdorfer *et al.*, Hyperfine Interact. **99**, 203 (1996).
[31] P. Beiersdorfer *et al.*, *X-ray Spectroscopy with EBIT*, in *UV*

and X-Ray Spectroscopy of Astrophysical and Laboratory Plasmas, edited by E. Silver and S. Kahn, (Cambridge University Press, Cambridge, 1993), p. 59 (Proceedings from the Tenth International Colloquium, Berkeley, CA, 1992).

[32] R.E. Marrs, *Atomic, Molecular, and Optical Physics: Charged Particles*, Vol. 29A of *Experimental Methods in the Physical Sciences* (Academic Press, San Diego, 1995), Chap. 14.

[33] P. Beiersdorfer and B.J. Wargelin, Rev. Sci. Instrum. **65**, 13 (1994).

[34] P. Beiersdorfer, J.C. López-Urrutia, E. Förster, J. Mahiri, and K. Widmann, Rev. Sci. Instrum. **68**, 1077 (1997).

[35] W.H. Bragg and W.L. Bragg, Proc. R. Soc. London, Ser. A **88**, 428 (1913).

[36] A. Burek, Space Sci. Instrum. **2**, 53 (1976).

[37] C.J. Borkowski and M.K. Kopp, Rev. Sci. Instrum. **39**, 155 (1968).

[38] P. Beiersdorfer *et al.*, Phys. Rev. A **53**, 3974 (1996).

[39] K. Reed (private communication).

[40] B.L. Henke, E.M. Gullikson, and J.C. Davis, At. Data Nucl. Data Tables **54**, 181 (1993) (data from this work can be found at www.cxro.lbl.gov).

[41] H.L. Zhang and D.H. Sampson, At. Data Nucl. Data Tables **43**, 1 (1989).

[42] A. Hibbert, M.L. Dourneuf, and M. Mohan, At. Data Nucl. Data Tables **53**, 23 (1993).

[43] R. Marrs, M. Levine, D. Knapp, and J. Henderson, Phys. Rev. Lett. **60**, 1715 (1988).

[44] A.J. Smith *et al.*, Phys. Rev. A **62**, 012704 (2000).

[45] J.A. Cogordan and S. Lunell, Phys. Scr. **33**, 406 (1986).